EMP Coupling to a Straight Conductor Above Ground: Transmission Line Formulation Based on Electromagnetic Reciprocity

R. G. Olsen, *Fellow, IEEE*, A.G. Tarditi, *Member IEEE*

***Abstract*-- A simple model for coupling of an electromagnetic plane wave incident on a conductor above ground has been developed using reciprocity theory, providing some advantages as compared to the conventional transmission line approach. The model is developed using a semi-infinitely long, single conductor above a lossy ground plane, and connected by an arbitrary load impedance to a vertical grounding conductor. This configuration corresponds to a worst-case wave coupling, because it leads to a line induced current larger than in the cases of finite and multiconductor lines. A frequency domain Thévenin equivalent model is developed to relate the incident wave amplitude to the voltage across a generic load, connected at any point on the vertical conductor. The application to the threat analysis of a High-altitude Electromagnetic Pulse (HEMP) impact on a power transmission line is discussed by considering the time domain solution (via inverse Fourier Transform) for an incident EMP fast-rise transient (E1) waveshape, following the standard IEC specifications. For typical high-voltage power line load impedances, it is shown that voltage magnitudes in the MV range can be induced across the line termination, in the case of a wave with near-grazing incidence angle, and with wave vector aligned along the horizontal conductor.**

***Index Terms*—Electromagnetic Pulse (EMP), Transmission Line Analysis, High Voltage Transmission Lines**

I. Introduction

A. Background

The possible consequences of a large-scale Electromagnetic Pulse (EMP) event on the electric power infrastructure has been studied for several decades, e.g. [1,2,3]. More recently, in part due to the ongoing modernization of the power grid, there has been a renewed interest in this matter, with specific focus towards the investigation of EMP risk-mitigation solutions related to the most critical grid assets [4].

In this context, a research effort sponsored by the US Department of Energy was initiated in 2016 [5], with the intent analyzing possible specific knowledge gaps related to the risk of EMP impact on high-voltage, power transformers (transmission-class), that indeed represent the most critical power grid assets. As a part of this initiative, this paper deals with the modeling of the fast-rise, initial transient of the EMP (typically referred to as E1 [6]) and, more specifically, focuses on an alternative formulation of the transmission line approach. for computing the voltage induced across the termination of a power line impacted by an E1 EMP component

This work is supported by the U.S. Department of Energy, Office of Electricity Delivery and Energy Reliability under contract number DE-AC05-00OR22725.
R. G. Olsen is with the School of EECS, Washington State University, Pullman, WA 99164-2752 USA , A. G. Tarditi is with Oak Ridge National Lab, Oak Ridge, TN, 37831 emails: bgolsen@wsu.edu; tarditiag@ornl.gov

B. Problem Statement

This work is focused on providing a quantitative estimate of E1 impact on a power line termination, for a realistic set of scenarios and for devising a guideline to assess the vulnerability of the grid components. While there are several possible configurations for transmission power lines, an important simplification can be made by considering the geometry that would lead to highest induced voltage or current on the line termination, for a given EMP illumination.

As has been shown in previous analyses [7-9], the case for a single, isolated perfectly conducting wire, with open circuit terminations, and without ground plane, leads to the maximum computed current induced by the EMP wave. The presence of a ground plane (both in the case of actual and ideal conductivity) and of other parallel wires provide some mitigation of the coupling from incident EMP.

For the present study, in order to provide relevant engineering estimates, the more realistic case of a single conductor over ground, with generic termination impedances, has been considered. In this context, the semi-infinitely long, open-circuit termination case, will provide the worst-case scenario, (*i.e.*, an upper limit for the EMP-induced termination voltage to ground, thus representing a conservative estimate from the perspective of EMP wave coupling). Using this model as a base, the induced voltage across a transformer input can be found by using a realistic input impedance for such a transformer.

C. Computational Approach

In principle, the calculation of the current induced on a conductor by an impinging electromagnetic wave of given characteristics can be done by solving the set of Maxwell equations along with the appropriate boundary condition specifications. For the case of a conductor parallel to an air-earth interface, this has been done for a variety of different cases and with a mix of analytic and numerical methods [10-12]: in particular, for applications to EMP-E1 coupling to power lines, the approximate solution via a transmission line approach is often considered, due to its simplicity and wide range of validity [13-15].

In the present study, a novel, electromagnetic-reciprocity based approach to the solution of wave coupling to a power line is presented, illustrating some inherent advantages and providing validation with previously published results.

II. Description of Problem and Solution Overview

The scenario under consideration is that of a semi infinitely long ($0 < z < \infty$) single conductor transmission line above earth illuminated by a single frequency ($\omega = 2\pi f$) plane wave and its reflection (Fig. 1). The transmission line consists of a horizontal conductor along the z-direction in the $x = 0$ plane augmented by an attached grounded vertical conductor. The line is loaded with a lumped impedance Z, located at a height $y = h_t$ along the vertical conductor. Each conductor is assumed to have a conductivity σ_w and a radius a. The earth is assumed to have a conductivity σ_2 and a relative permittivity ε_{r2}. Free space is represented by permittivity and permeability ε_0 and μ_0 respectively. Finally, the vertical conductor extends into the earth a distance h_g and the portion below the surface must be accounted for in the solution.

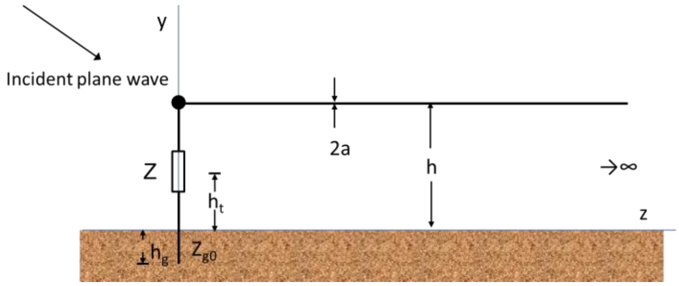

Fig. 1. Geometry of the problem

The solution approach consists in first removing the impedance Z leaving an open circuit at height h_t, as shown in Fig. 2. Then a Thévenin equivalent circuit at these terminals (shown in Fig. 3) is identified, thus including the incident and reflected plane wave, and the open-circuited, semi-infinite transmission line. The open circuit voltage of this Thévenin equivalent is found using reciprocity theory. In parallel with this, the Thévenin impedance is found. Once this equivalent circuit has been identified, the voltage across and current through the impedance Z can easily be found.

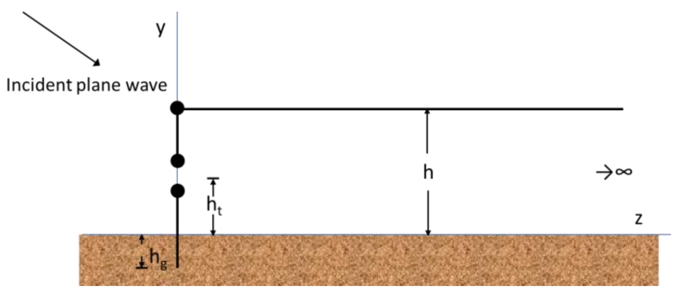

Fig. 2. System with termination impedance removed.

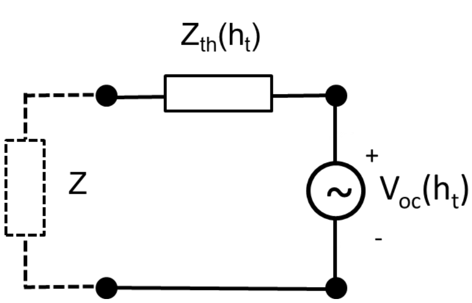

Fig. 3. Thévenin equivalent for the system with termination impedance (Z) shown.

III. Reciprocity Solution – frequency domain

A. General Frequency Domain Solution

A linear isotropic system (not necessarily electrically small) with two pairs of terminals (Ports) 1 and 2 is considered, as shown in Fig. 4. If "Problem a" and "b" represent two different sets of voltage or current sources for the same system, it is known from reciprocity theory that [16,17]

$$V_{1a}I_{1b} + V_{2a}I_{2b} = V_{1b}I_{1a} + V_{2b}I_{2a} \tag{1}$$

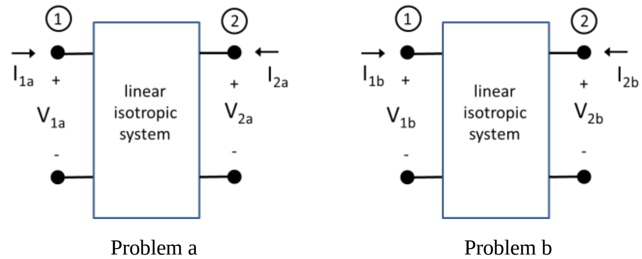

Fig. 4. Arbitrary linear isotropic system with two pairs of terminals (Ports) with voltages and currents defined at Port 1 and Port 2.

At this point, the two specific problems to be used in the reciprocity solution are shown in Fig. 5 and will be described here. Each involves the same linear, isotropic system with two ports. The first port is on a vertical wire at $z = 0$ and height h_t while the second is on a horizontal wire of height h at a distance z to the right of the vertical wire or at some height y along the vertical wire.

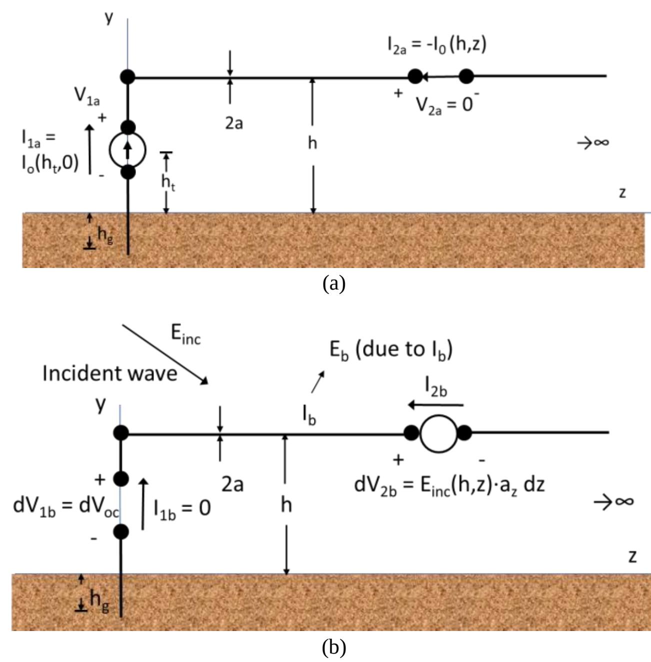

Fig. 5. Problems to which reciprocity theory will be applied to identify a Thévenin equivalent circuit

The first problem in Fig. 5a corresponds to "Problem a" in Fig. 4 with its Port 1 driven by a current source of amplitude $I_{1a} = I_0(h_t, 0)$ and Port 2 on the horizontal wire at z (or on the vertical wire at height y) short circuited so that $V_{2a} = 0$. The voltage across Port 1 is V_{1a} while the current into Port 2 is $I_{2a} = -I_0(h, z)$. The minus sign is needed because the reference directions for I_{2a} and $I_0\left(h,z\right)$ are in opposite directions. The second problem in Fig. 5b shares the same geometry as that of Fig. 5a but is excited by an external wave $\bar{E}_{inc}$ (incoming plane wave and reflected wave) that satisfies air-earth boundary conditions at $y = 0$ and induces a current I_b on the wire which is open circuited at Port 1 so that $I_{1b} = 0$. The current I_b induced on the wire causes an additional electric field $\bar{E}_b$ that again satisfies the air-earth boundary conditions at y = 0. The total voltage across Port 2 (of length $d\bar{\ell}$) due to the total axial electric field is

$$(\bar{E}_{inc}\left(h,z\right)+\bar{E}_b(h,z))\cdot d\bar{\ell}=0 \tag{2}$$

and is equal to zero if the wire is a perfect electric conductor. However, this derivation can be generalized to wires with a finite intrinsic impedance per unit length, z_{iw} with the same result since terms containing z_{iw} cancel. Note that the absence of a minus sign in (2) is due to the choice of reference directions for the voltage and the electric field. The specific "Problem b" of Fig. 4b will now be described. The specific source for this problem is the portion of the induced current I_b between the terminals of Port 2. Given (2), the voltage across Port 2 can be written as $dV_{2b}=\bar{E}_b\left(h,z\right)\cdot\bar{a}_z dz=-\bar{E}_{inc}\left(h,z\right)\cdot\bar{a}_z dz$ and a corresponding voltage dV_{1b} (i.e., the open circuit voltage dV_{oc} due to the Port 2 source current) can be identified across Port 1. It should be noted that each voltage is "differential" because the Port 2 gap is infinitesimal while the incident electric field is finite.

The problem illustrated in Fig. 5a (i.e., "Problem a") can be solved in a straightforward manner for arbitrary frequencies using either numerical techniques or analytical techniques appropriate for the high frequency regime [18]. Later simple explicit solutions for lower frequencies will be given, but here it will be assumed that the current through Port 2

$$I_{2a}=-I_0\left(h,z\right) \tag{3}$$

can be found.

It is not actually necessary to directly solve for the currents and voltages in the circuit of Fig. 5b (i.e., "Problem b") . In fact, one advantage of the approach here introduced is that solving this relatively complicated electromagnetic scattering problem can be avoided. Rather, the open circuit voltage in "Problem b" (the original goal) will be found using reciprocity.

Since $V_{2a}=0$ and $I_{1b}=0$, (1) reduces to

$$0=dV_{1b}I_{1a}+dV_{2b}I_{2a} \tag{4}$$

or equivalently

$$0=dV_{oc}\left(h_t\right)I_0\left(h_t,0\right)+\bar{E}_{inc}\left(h,z\right)\cdot\bar{a}_z dz I_0\left(h,z\right) \tag{5}$$

If now, (5) is solved for the open circuit voltage and (3) inserted into the result (for the horizontal wire)

$$dV_{oc}\left(h_t\right)=-\left(I_0\left(h,z\right)/I_0\left(h_t,0\right)\right)\bar{E}_{inc}\left(h,z\right)\cdot\bar{a}_z dz \tag{6}$$

Finally, since (6) is only the result for the portion of the incident field at a point "z", it must be integrated over sources at all points on the wire including those on the vertical wire. The result is

$$\begin{aligned}V_{oc}\left(h_t\right)=&-\frac{1}{I_0\left(h_t,0\right)}\int_{-h_g}^{h}I_0\left(y,0\right)\bar{E}_y\left(y,0\right)dy\\&-\frac{1}{I_0\left(h_t,0\right)}\int_0^{\infty}I_0\left(h,z\right)\bar{E}_{inc}\left(h,z\right)\cdot\bar{a}_z dz\end{aligned} \tag{7}$$

The contribution of the wire in the earth has been included in (7). However, it can often be neglected at lower frequencies because the vertical electric field in the earth (E_{earth}) is very small compared to that in the air (E_{air})by the boundary condition $E_{earth}\cong(j\omega\varepsilon_0/\sigma_2)E_{air}$ while the current is continuous across the boundary. Also, between the terminals of Port 1 the total electric field is much larger than $\left|\bar{E}_{inc}\right|$ because the scattered electric field is concentrated around open circuited terminals as in a receiving antenna. Hence it is not necessary to add $\bar{E}_{inc}$ in calculating the total open circuit voltage.

While solving "Problem a" the Thévenin impedance can be determined by dividing the voltage $V\left(h_t\right)=V_{1a}$ across the Thévenin terminals by the current source amplitude, $I\left(h_t,0\right)$ when the current source is connected to Port 1.

$$Z_{th}\left(h_t\right)=V_1\left(h_t\right)/I\left(h_t\right) \tag{8}$$

From Fig. 3, the current through the impedance Z can be written as

$$I_Z\left(h_t\right)=V_{oc}\left(h_t\right)/\left(Z_{th}\left(h_t\right)+Z\right) \tag{9}$$

and the voltage across the impedance is simply

$$V_Z\left(h_t\right)=I_Z\left(h_t\right)Z=V_{oc}\left(h_t\right)Z/\left(Z_{th}\left(h_t\right)+Z\right) \tag{10}$$

To this point, the solution (7) is valid for any frequency as long as i) the appropriate current distribution is used and ii) the gap across which $V_{oc}\left(h_t\right)$ is defined is small compared to the wavelength of the incident wave; no voltages are defined for which the spacing between terminals is comparable to or larger than a wavelength.

The motivation for using reciprocity theory to solve a problem that has been previously solved using field coupled transmission line theory [19], can be highlighted as follows:

1. The use of reciprocity theory eliminates the need to solve a relatively more difficult problem (i.e., that of the problem in Fig. 5b) that involves electromagnetic scattering, to find a current distribution on the conductors.
2. No voltages need to be defined (thus no reference zero potential is required) except those between closely spaced terminals, for which the voltage is unique and well defined. This is important because the voltage between the line and ground is strictly unique only when the condition h << λ is satisfied
3. By proper selection of currents in (7), the solution can be used at higher frequencies than in methods that are based on the transmission line approximation. For example, a current such as that in [20] might be used.
4. Since the system modelled by the Thévenin equivalent is linear, the equivalent circuit can be used to solve for the current in a non-linear load such as has been done in [19,21].

B. The Incident Wave Electric Field

The incident electric field consists of a vertically polarized plane wave and its reflection in the *yz* plane. The relevant axial (e.g., along "z") electric field is

$$E_z(x,y,z) = E_{zv}(x,y)e^{-jk_0 z\cos\psi} \quad (11)$$

where

$$E_{zv}(x,y) = E_v \sin\psi\left(e^{jk_0 y\sin\psi} - R_v e^{-jk_0 y\sin\psi}\right) \quad , \quad (12)$$

E_v is the amplitude of the incident wave, and the geometry for this incident wave is shown in Fig. 6 [8]. Reference [8] also has a more general incident plane wave. R_v is the reflection coefficient for the vertically polarized field expressed as

$$R_v = \frac{(\varepsilon_{r2}+\sigma_2/j\omega\varepsilon_0)\sin\psi - \left[(\varepsilon_{r2}+\sigma_2/j\omega\varepsilon_0)-\cos^2\psi\right]^{1/2}}{(\varepsilon_{r2}+\sigma_2/j\omega\varepsilon_0)\sin\psi + \left[(\varepsilon_{r2}+\sigma_2/j\omega\varepsilon_0)-\cos^2\psi\right]^{1/2}} \quad (13)$$

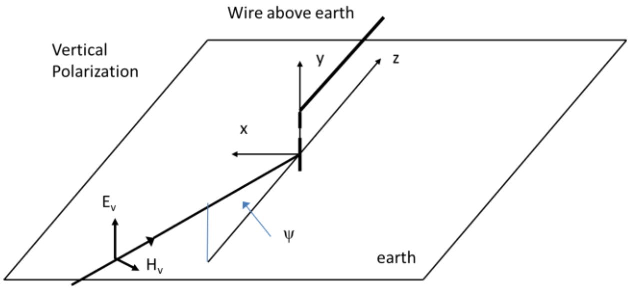

Fig. 6. Geometry of the incident plane wave and its reflection for ϕ = 0. The transmission line is absent for this calculation.

The vertical electric field of the incident plane wave is

$$E_y(x,y,z) = E_y(x,y)e^{-jk_0 z\cos\psi\cos\phi} \quad (14)$$

where

$$E_y(x,y) = E_v\cos\psi\left(e^{jk_0 y\sin\psi} + R_v e^{-jk_0 y\sin\psi}\right)e^{jk_0 x\cos\psi\sin\phi} \ . \quad (15)$$

C. Reduction to the Low Frequency Limit

If it is now assumed that $h \ll \lambda$, the problem illustrated in Fig. 5a (i.e., "Problem a") can easily be solved using the equivalent transmission line theory for a wire above earth, since the wire is driven through electrically short vertical wires by a current source at its left end [22]. The result is

$$I_0(h,z) \cong I_0(h_t,0)e^{-j\gamma_{TL}z} \quad (16)$$

where the propagation constant γ_{TL} is given in Appendix A. From (7), using $h \ll \lambda$ for the first integral and (16) with $I_0(h,0) \cong I_0(h_t,0)$ for the current, it is found

$$V_{oc}(h_z) = V_{oc1} + V_{oc2} \cong -h\bar{E}_y(h/2) - \int_0^\infty e^{-j\gamma_{TL}z}\bar{E}_{inc}(h,z)\cdot\bar{a}_z dz \quad , \quad (17)$$

where the vertical electric field is evaluated at half the height of the horizontal wire although the specific height is arbitrary since the vertical electric field is relatively constant along the vertical wire.

The Thévenin impedance can be determined while solving "Problem a" with reference to the circuit shown in Fig. 7. Here the current source $I(h_t,0)$ connected to the input terminals is in series with the grounding impedance Z_{g0} shown as the buried wire in Fig. 1 and the input impedance Z_{in} of the semi-infinite wire above earth transmission line. This impedance is simply the characteristic impedance Z_{0TL} of the wire above earth equivalent transmission line and is given in Appendix A. For this derivation, Z_{g0} at low frequencies can be determined using standard quasi-static techniques or high frequency models discussed in [23,24].

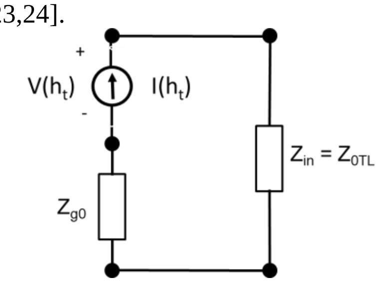

Fig. 7. Input Circuit for Conductor above the Earth Transmission Line. The source is at $y = h_t$.

Given this background, the Thévenin impedance for the equivalent circuit in Fig. 3 is

$$Z_{th}(h_t) = Z_{g0} + Z_{0TL} \quad (18)$$

D. Calculating the Low Frequency Thévenin Equivalent

The open circuit voltage in (17) will now be evaluated using the incident field given in the previous section. To begin, since the current on the vertical wire has been assumed to be constant, the term V_{oc1} simply becomes

$$V_{oc1} \cong -E_v h(1+R_v)\cos\psi \quad (19)$$

In a subsequent paper, the constant current assumption will be relaxed and the current on the vertical wire allowed to be a function of the distance above the earth.

Next, using (16), (17) and (11) with x = 0, the contribution of the horizontal conductor can be written as

$$V_{oc2} = -E_{zv}(0,h)\int_0^\infty e^{-jk_0 z\cos\psi}e^{-j\gamma_{TL}z}dz \quad (20)$$

where $E_{zv}(0,h)$ is defined in (12). This integral can be evaluated analytically (assuming, in general, that the imaginary part of γ_{TL} is nonzero) and (20) becomes

$$V_{oc2} = \frac{jE_{zv}(0,h)}{(k_0\cos\psi + \gamma_{TL})} \quad (21)$$

Hence, the open circuit voltage is the sum of (19), and (21):

$$V_{oc} = -E_v h(1+R_v)\cos\psi + \frac{jE_{zv}(0,h)}{(k_0\cos\psi + \gamma_{TL})} \quad (22)$$

As shown earlier, the Thévenin impedance is given in (18).

E. Validity of the Low Frequency Result

As shown in Appendix B, that the open circuit voltage in (22) reduces to the expression from [19] derived from the solution of the telegrapher's equations.

Furthermore, the simple result given in (22) is generally valid for frequencies such that h << λ, or f(MHz) $<< 300/h$ (meters). In the specific case for a HEMP standard waveform, it is expected be valid over a wide enough range of frequencies to calculate worst-case induced voltages for the following reasons. Specifically, the first term in (22) (i.e., V_{oc1}) can be ignored if two important criteria are satisfied. First, if $h_t = 0$ (as assumed for the results in this paper) there are no problems with high frequency resonances which can occur for wire lengths greater than a quarter wavelength and can cause V_{oc1} to become large. Second, it is shown in Section IV and validated numerically that the second term of (22) dominates the first in the case of near-grazing incidence. Since this case produces the largest line termination voltages (i.e., the worst-case scenario), the validity of V_{oc2} over the entire frequency range relevant to the EMP becomes an important issue. The only assumption made in deriving (21) is the that of the wire over earth equivalent transmission line current, as in (16). This current is valid at low frequencies, but also can be shown to be in good approximation equivalent to the current on thin lossless wires in free space (i.e., $I\exp(-jk_0 z)$) when the frequency becomes sufficiently high [25]. In this case then (21) can be accurate enough at higher frequencies, while considering a small amount of loss due to the conducting wire that is required for convergence, and (15) for the electric field.

For the Thévenin impedance generally, $Z_{0TL} >> Z_{g0}$. Hence the relevant question is whether Z_{0TL} is accurately represented by the characteristic impedance of the equivalent transmission line over the frequency range of the HEMP standard waveform. As it was verified, the analysis of the transfer function of the linear system that represents coupling of the EMP pulse to a transformer at the end of a semi-infinite power line at height h = 10 meters (the case considered here) indicate that frequencies higher than approximately 5 MHz are attenuated. Further, it has been shown that the transmission line approximation is reasonably valid (for h = 10 meters) up to 5 MHz [20]. Hence, it is can be concluded that the Thévenin impedance is reasonably valid over the range of frequencies relevant to this problem.

IV. Discussion of the Worst-Case Frequency Domain Result (Grazing Incidence)

From (21) it can be noted that V_{oc2} becomes large for plane waves at angles of incidence such that $k_0\cos\psi + \gamma_{TL} \cong 0$. Generally, this occurs for angles near grazing incidence, from the right of Fig. 1 (i.e., $\cos\psi \cong -1$ in Fig. 5) and results in a significantly pulse enhanced coupling to the conductor (and then to its load). From (13), it is also clear that E_{zv} vanishes for $\psi \cong \pi$, however a detailed analysis of (21) shows that V_{oc2} reaches a maximum value at an angle ψ_{max}, as ψ approaches π [26]. It can be shown that this maximum also occurs for finite line lengths, and the longer the line, the closer ψ_{max} gets to π, that is V_{oc2} peaks closer to grazing incidence conditions.

This result was analyzed by first considering that the impact of the incident field on the conductor can be represented by a set of distributed voltage sources (as in [18], [27]). These sources represent the voltage $dV_s(z_s)=E_s(z_s)dz$ on each infinitesimal segment dz of the line that is induced from the external (incident plus reflected) field $E_s(z_s)$ in z = z_s. Each source also generates traveling waves along the conductor: for example, similarly to (16), let $dV_{line}(0, z_s) = e^{j\gamma_{TL} z_s} dV_s(z_s)$ be the transmission line voltage in $z=0$ (with zero reference to infinity, for a semi-infinite line) from a source $dV_s(z_s)$ in $z=z_s$. The total line voltage will be then found by integrating the $dV_{line}(0, z_s)$ contributions, for each z_s ranging from 0 to ∞. This total line voltage corresponds to V_{oc2} in (21), as it is may be deducted from the discussion in Appendix B.

One could consider an approximate distribution of finite voltage sources $V_n=V_s(z_n)=E_s(z_n)\Delta z$ *defined* over segments of the line of length Δz and centered in z = z_n. Then the total line voltage can be approximated with the series

$$V(0) \cong \sum_{n=0}^{N} V_{line}(0, z_n) = \sum_{n=0}^{N} e^{j\gamma_{TL} z_n} V_s(z_n) = \sum_{n=0}^{N} e^{j\gamma_{TL} z_n} E_s(z_n)\Delta z$$

that converges to the integral V_{oc2} for N→∞ and Δ →0.

By analyzing the terms of the series, it can be shown that the traveling wave contributions $V_{line}(0, z_n)$ add up both with a larger amplitude, and with smaller phase spread when ψ approaches ψ_{max}. On the other hand, for ψ away from ψ_{max}, these contributions have lower amplitudes and/or an increased phase spread, thus leading lower cumulative effect [28].

This effect of a larger induced voltage at near-grazing incidence is know from previous analyses of EM wave coupling on long conductors (e.g. [9, 26]), and it also represents the fundamental physics behind the Beverage receiving antenna [25].

V. The Time Domain Response

This section presents the application of the TL model in the time domain. The incident waveform is considered according to the IEC-E1 standard [6] as

$$\begin{aligned} E_v(t) &= 0, & t<0 \\ & E_{01}k_1\left(e^{-a_1 t} - e^{-b_1 t}\right), & t>0 \end{aligned} \qquad (23)$$

where

$$E_{01} = 50,000\, V/m, \quad k_1 = \left(\frac{b_1}{b_1 - a_1}\right)\left(\frac{b_1}{a_1}\right)^{\frac{a_1}{b_1 - a_1}} = 1.3,$$

$$a_1 = 4x10^7 \sec^{-1}, \quad b_1 = 6x10^8 \sec^{-1}$$

. The Fourier transform of this waveform is

$$E_v(\omega) = E_{01}k_1 e^{-j\omega t}\left(\frac{b_1 - a_1}{(a_1 + j\omega)(b_1 + j\omega)}\right) \qquad (24)$$

The waveform in (23) has rise and fall times of approximately 5 and 60 ns, respectively. The Fourier transform (24) was multiplied by the voltage across an arbitrary impedance Z in (10) (together with (12) and (12)-(14), and (18) with Z_{g0} set to zero), then sampled and transformed into the time domain using the inverse Fourier Transform. Several comments will be made before presenting the results.

First, the solution was (partially) validated by comparing the calculated value of V_{oc} for the special case of perfectly conducing earth and h << λ. As shown in Appendix C, the result for V_{oc} should be equal to $-2hE_v$. Since this is a constant, it was verified that in this case the time domain response indeed corresponds to the waveshape (23) multiplied by $-2hE_v$.

Second, the low frequency range of (22) is important for calculating the long-term time response. Here, however, the results shown in Figs. 8 i and 9 were generated by calculating the inverse transform of (10), using (22), (18) and the capacitive load impedance. The finite number of samples used produces a small offset voltage which tends to zero as the number of samples was increased, thus it has been subtracted from the result. Finally, while any load (including nonlinear ones) could be used for the calculations of termination voltage, either a 100 pF or 300 pF capacitive load was considered. These choices were made because measurements of typical load impedances of transformer bushings or surge arresters in high-voltage lines give values of capacitance between 100 and 300 pF.

VI. Results

Using the IEC input pulse waveform (23) for the incident field, the voltage across the terminals shown in Fig 1 was computed for a capacitive load impedance and with the physical parameters in Table I, while the FFT used 128K samples with a value of the largest time sample for the inverse Fourier transform equal to 10 µsec. The results are shown in Figs. 8 and 9.

Wire/Earth		Geometry		Incident field/ loads	
σ_w (S/m)	3.5x10^7	a (m)	.01	Z_{g0} (Ω)	5
σ (S/m)	0.01	h (m)	10	C_t (pF)	text
ε_r	5	h_t (m)	0	E_v (V/m)	1.0
		ϕ (rad)	0	E_h (V/m)	0.0

Table I. Parameters used for calculation of transient voltages in Figs. 8 - 9.

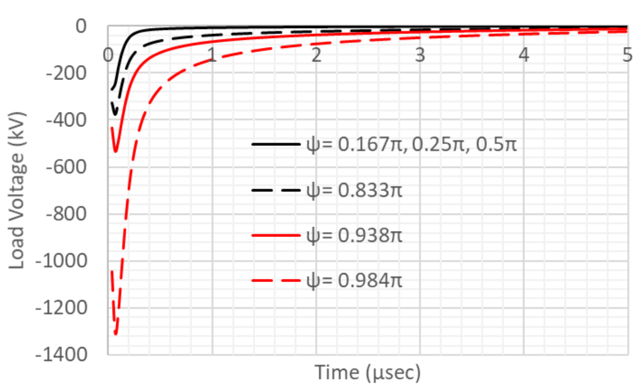

Fig. 8. Load voltage across a 100 pF capacitor at the junction of a semi-infinite horizontal single conductor transmission line and a vertical riser at its end due to an incident IEC-E1 pulse, and with the parameters given in Table I.

It is shown in Fig. 8 that, aside from the grazing incidence cases, the load voltage for the 100 pF case *i)* is roughly independent of incidence angle i*i)* becomes spread out over a few microseconds and *iii)* reaches a maximum magnitude of about 200 kV. As expected, and discussed in section IV-A, however, the magnitude of the load voltage increases as the angle of incidence approaches grazing. In this case, the maximum load voltage can reach about 1 MV. For the 300 pF case of Fig. 9, as expected, the maximum voltage magnitude is lower, limited to about 100 kV for large incidence angles, and to approximately 800 kV for near-grazing incidence. It has been verified that for larger transmission line heights, these voltages can be expected to increase.

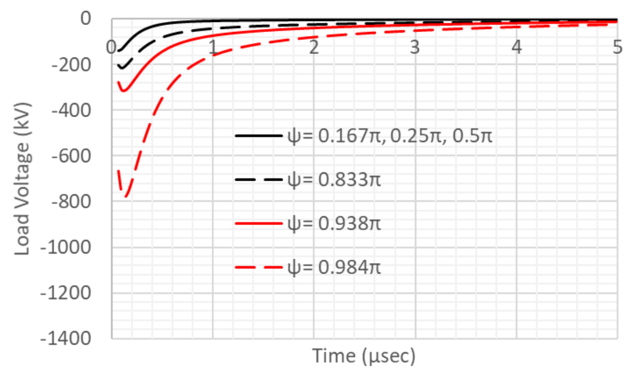

Fig. 9. Load voltage across a 300 pF capacitor at the junction of a semi-infinite horizontal single conductor transmission line and a vertical riser at its end due to an incident IEC pulse, and with the parameters given in Table I.

VII. Conclusions

A model for the coupling of the fast-rise component of a High-altitude Electromagnetic Pulse (HEMP) to a transmission power line has been developed using the electromagnetic reciprocity principle. The model has been validated by comparing it to the traditional approach based on transmission line theory with a distributed voltage source excitation.

Time-domain results for the solution of the voltage across a typical high voltage power line load impedance (such as a transformer bushing) have been derived by considering the impact of a plane wave on a single, semi-infinitely long conductor line above a lossy ground plane. This provides an illustration of the worst-case condition for the surge voltage that can be generated on an actual power line termination. It was found that the maximum voltage across the load can reach magnitudes in the MV range , for near-grazing wave incidence conditions. Transmission lines higher than 10 m have been verified to have larger induced voltages.

While the geometry considered for this analysis is limited to conditions for which the line height is electrically small as compared to the incident wavelength, extensions to a more general case that includes higher frequencies, as well as to responses in presence of non-linear loads, can be developed in a straightforward manner and will be discussed in a follow-up publication.

VIII. References

1. Legro, J. et. al., "Study to Assess the Effects of High Altitude Electromagnetic Pulse on Electric Power Systems, Phase I Final Report", Oak Ridge National Laboratory Report, ORNL/Sub/8643374/1/V2, 1986
2. Barnes, P. R. et al., *Electromagnetic Pulse Research on Electric Power Systems: Program Summary and Recommendations* ORNL/Sub/85-28611/2, 1993
3. Burrage, L. M. et al. Impact of Steep-Front Short-Duration Impulse on Electric Power System Insulation Phase II: Laboratory Evaluation of Selected Power System Components, ORNL/Sub/85-28611/2, 1991.
4. Foster, J. S. Jr. et. al. *Report of the Commission to Assess the Threat to the United States from Electromagnetic Pulse (EMP) Attack, Critical National Infrastructures*, Presidential EMP Commission, April, 2008.
5. Tarditi, A. G. et. al. , Devices and Integrated Systems Posters, p. 10, 2017 Grid Modernization Initiative Peer Review Meeting, Washington, DC, April 18, 2017
6. IEC, "Electromagnetic compatibility (EMC) – Part 2: Environment – Section 9: Description of HEMP environment – Radiated disturbance,

Basic EMC Publication," IEC 61000-2-9, February 1996, International Electrotechnical commission, Geneva, Switzerland.
7. Lee, K. S. H., Summa Interaction Note 435, 1983.
8. Tesche, F. M. and P. R. Barnes, A Multiconductor Model for determining the Response of Power Transmission and Distribution Lines to a High Altitude Electromagnetic Pulse (HEMP). *IEEE Trans.* Vol PWRD-4. pp. 1955-1964, July 1989
9. Neff, H. P. and D. A. Reed, "The Effect of Secondary Scattering on the Induced Current in a Long Wire Over an Imperfect Ground from an Incident EMP", *IEEE Trans,* Vol AP-31, pp 1554-1558, Dec. 1989.
10. P. R. Barnes, "The Axial Current Induced on an Infinitely Long, Perfectly Conducting, Circular Cylinder in Free Space by a Transient Electromagnetic Plane Wave", EMP Interaction Notes, Note 64, 1971 http://ece-research.unm.edu/summa/notes/In/0064.pdf
11. Lee, K.S.H, et al. "Interaction of High-Altitude Electromagnetic Pulse (HEMP) with Transmission Lines: An Early-Time Consideration", Interaction Notes, Note 435, 1983 http://ece-research.unm.edu/summa/notes/In/0435.pdf
12. G. E. J. Bridges and L. Shafai, "Plane wave coupling to multiple conductor transmission lines above a lossy earth", *IEEE Trans*, Vol. EMC-31, No. 1, pp. 21-33, Feb 1989. doi: 10.1109/15.19904
13. W. Scharfman, E. Vance and K. Graf, "EMP coupling to power lines", in *IEEE Trans.*, Vol. APS-26, no. 1, pp. 129-135, January 1978.
14. Vance, E. F., *Coupling to shielded cables,* Wiley, 1978
15. F. M. Tesche, "Comparison of the transmission line and scattering models for computing the HEMP response of overhead cables", *IEEE Trans.*.Vol. EMC-34, no. 2, pp. 93-99, May 1992
16. Weeks, W. L. *Antenna Engineering* , McGraw Hill, New York, 1968
17. Van Valkenburg, M. E. and J. B. Cruz, *Signals in Linear Systems*. Houghton Mifflin, Boston, 1974.
18. Olyslager, F., *Electromagnetic Waveguides and Transmission Lines*, Oxford University Press, Oxford, 1999
19. Tesche, F. M., M. Ianoz and T. Karlsson, *EMC Methods and Computational Models*. Wiley Interscience, New York 1997
20. Chang, D. C. and R. G. Olsen, "Excitation of an Infinite Antenna Above a Dissipative Earth", *Radio Science*, Vol. 10, Nos. 8-9, pp. 823–832, August–September 1975
21. R. G. Olsen and K. Yamazaki, "The Interaction Between ELF Electric Fields and RF Survey Meters: Theory and Experiment", *IEEE Trans.*, Vol. EMC-47, No. 1, pp. 86-96, Feb. 2005
22. Olsen, R. G. and T. A. Pankaskie, "On the Exact, Carson and Image Theories for Wires at or Above the Earth's Interface", *IEEE Trans.* Vol. PAS-102, No. 3, pp. 769–774, March 1983.
23. He, J. R. Zeng and B. Zhang, *Methodology and Technology for Power System Grounding,* Wiley, New York, 2013
24. Grcev, L. and M. Popov, "On High-Frequency Circuit Equivalents of a Vertical Ground Rod", *IEEE Trans*. Vol. PWRD-20. pp. 1598-1603. April. 2005.
25. Krause, J. D. *Antennas*, 2nd Ed. McGraw Hill 1988
26. Olsen, R. G. and D. C. Chang, "Current Induced by a Plane Wave on a Thin Infinite Wire Near the Earth", *IEEE Trans.* Vol. AP-22, No. 4, pp. 586–589, July 1974.
27. Tesche, F. M., "Plane Wave Coupling to Cables,", Part II, Chapter 2 in *Handbook of Electromagnetic Compatibility,* R. Perez, ed., Academic Press, 1995
28. A. G. Tarditi, A. G. and R. G. Olsen, "Incidence Angle Impact on EM Wave-Line Coupling ", submitted to the 2018 American Electromagnetics (AMEREM) Conference, Santa Barbara, CA (USA), August 27-31, 2018

IX. Biographies

Robert G. Olsen (S'66, F'92) received the BSEE degree from Rutgers University, New Brunswick, NJ in 1968 and the MS and Ph.D. degrees from the University of Colorado, Boulder, CO in 1970 and 1974 respectively.

He has been with Washington State University since 1973. Other positions include Senior Scientist at Westinghouse Georesearch Laboratory, NSF Faculty Fellow at GTE Laboratories, Visiting Scientist at ABB Corporate Research and EPRI and Visiting Professor at the Technical. University of Denmark.

His research is the application of electromagnetic theory to high voltage power transmission systems and has resulted in 90 and 150 publications in refereed journals and conferences. He is one author of the *AC Transmission Line Reference Book – 200 kV and Above* which is published by EPRI.

He is a Life Fellow of the IEEE, an Honorary Life member of the IEEE Electromagnetic Compatibility (EMC) Society. He is also past chair of the IEEE Power Engineering Society AC Fields and Corona Effects Working Groups. In addition, he is past Associate Editor of the *IEEE Transactions on Electromagnetic Compatibility* and *Radio Science*.

Alfonso G. Tarditi (M '07) completed his academic education at the University of Genoa, in Genoa, Italy (B.S. and M.S. in Electronics Engineering, 1985, Doctorate in Electrical Engineering, 1990). In the next two years he was awarded a N.A.T.O. post-doctoral fellowship at UC Berkeley. Since that time he was involved in fusion research, that continued first after joining the Lawrence Livermore National Laboratory, and then with Science Application International Corporation.

He then held positions as Sr. Scientist with contractors at the NASA Johnson Space Center (Houston, TX), leading R&D in electromagnetic compatibility, and in space propulsion and power systems. During that time, he also taught Plasma Physics and Electrodynamics at the University of Houston. After serving as a project manager at the Electric Power Research Institute, and as Chief Scientist at NPL Associates Inc. (Urbana, IL), focused on plasma and nuclear technologies, he joined the Senior R&D staff at the Oak Ridge National Laboratory.

Appendix A

Wire Above Earth Equivalent Transmission Line

Expressions for the relevant parameters of a transmission line equivalent to the wire over the earth problem at low frequencies are given here [19].

$$\gamma_{TL} = \pm j\sqrt{z_{11}y_{11}} \cong \pm\left(k_0^2\left(1-\frac{J_c(a,h,h)}{\ln(2h/a)}\right)-\frac{j2\pi\omega\varepsilon_0 z_{iw}(\omega)}{\ln(2h/a)}\right)^{1/2},\ \mathrm{Im}(\gamma_{TL})\le 0 \quad \text{(A1)}$$

is the propagation constant for the horizontal wire above ground where

$$z_{11} \cong \frac{j\omega\mu_0}{2\pi}\left\{\ln(2h/a) - J_c\left(a,h,h\right)\right\} + z_{iw} \quad \text{(A2)}$$

is the series impedance of the conductor above earth, and $J_c\left(a,h,h\right)$ is the Carson integral defined as

$$J_c\left(a,h,h\right) = \frac{2}{k_2^2}\int_0^\infty \left(u-\kappa\right)e^{-2h\kappa}\cos\left(\kappa a\right)d\kappa \quad \text{(A3)}$$

$u=\sqrt{\kappa^2-k_2^2}$, $k_2 \cong \mathrm{e}^{-j\pi/4}\sqrt{\omega\mu_0\sigma_2}$ if $\sigma_2 >> \omega\varepsilon_0\varepsilon_{r2}$.

In (A2) z_{iw} is the intrinsic impedance per unit length of the conductor:

$$z_{iw} = r + j\omega l_i = r_{dc}\left(k_w a/2\right)J_0\left(k_w a\right)/J_1\left(k_w a\right) \quad \text{(A4)}$$

where

$$r_{dc} = 1/\left(\sigma_w \pi a^2\right) \quad \text{(A5)}$$

is the resistance per unit length of the wire at *dc* (i.e., zero frequency), σ_w is the wire conductivity, $k_w = \left(-j\omega\mu_0\sigma_w\right)^{1/2}$ and $J_0\left(k_w a\right)$ and $J_1\left(k_w a\right)$ are Bessel functions of argument *q*, and order zero and one, respectively. Low and high frequency approximations to z_{iw} are available [15].

The admittance per unit length is

$$y_{11} \cong 2\pi j\omega\varepsilon_0\left\{\ln(2h/a)\right\}^{-1} = j\omega c \quad \text{(A6)}$$

where the capacitance per unit length is defined as

$$c = 2\pi\varepsilon_0/\ln\left(2h/a\right) \quad \text{(A7)}$$

Since the horizontal conductor is semi-infinitely long, there is no reflected wave from the right side and the input impedance is simply the characteristic impedance of the wire above earth. This impedance is

$$Z_{th} = Z_{0TL} = \sqrt{z_{11} / y_{11}} \tag{A8}$$

Appendix B

Comparison to Distributed Voltage Source Excitation Theory

Given that the reciprocity-based derivation is not a traditional approach to the problem of an EM wave incident on conductors, it is important to validate the results by comparison to more traditional methods [17] or [23].

The distributed voltage source excitation theory is discussed for a generic transmission line illuminated by an incident plane wave in [17], Fig. 7.17. Further, the validation will be performed for a generic line length L, showing that it holds also for $L \rightarrow \infty$. Without limiting generality, it will be assumed that, in reference to Fig. 2, $h_t \cong h$ (an infinitesimal gap distance), so that the gap is at the top of the vertical conductor (although, as long as $h << \lambda$, the final result is independent of the exact value for h_t). The validation holds for both PEC and lossy ground and conductor conditions, the only difference being in the actual values used for Z_{0TL} the and γ_{TL}. Finally, to be consistent with notation of this paper, x and z in [17] will be replaced by z and y respectively, E_0, d and k in [17] will be set equal to E_v, h and k_0 respectively, and instead of γ in [17], $-j\gamma$ will be used, consistently with (16).

The solution in [17] is provided through the BLT equations, a compact version of the telegraphers' equation solution written as in [17, eq. (6.42)] for the voltages and currents at the a line terminations with generic impedances Z_1 at z=0, and Z_2 at z=L. The same equations can be formulated for the case of distributed source, referring to the case of a line illuminated by an incident wave, as in [17, eq. 7.35], and from that, with the present notations, the termination voltage V(z) at z=0 can be written as

$$V(0) = -\frac{e^{jL\gamma} S_2 (1+\rho_1)}{-e^{2jL\gamma} + \rho_1 \rho_2} - \frac{S_1 (1+\rho_1)\rho_2}{-e^{2jL\gamma} + \rho_1 \rho_2} \tag{B1}$$

where S_1 and S_2 are source terms that depend on the incident field and ρ_1 and ρ_2 are the line termination reflection coefficients.

For the purpose of this comparison, $Z_1 \rightarrow \infty$ (i.e., the input terminals are open-circuited in the same way as the problem described earlier in Fig. 1). Also, in order to represent the semi-infinite line condition, Z_2 will be set to the characteristic impedance of the transmission line, so that there is no reflected wave. With these assumptions then ρ_1=1 and ρ_2=0 and (B1) simplifies as

$$V(0) = 2e^{-jL\gamma} S_2 \tag{B2}$$

where

$$S_2 = -\frac{1}{2}\int_0^L e^{j\gamma(L+\zeta)} V_S'(\zeta) d\zeta + e^{jL\gamma}\frac{V_1}{2} - \frac{V_2}{2} \tag{B3}$$

In (B3), V_S' is the distributed voltage source along the wire which is related to the external field along the line E_z, at the height "y=h" from the ground). This is the z-component of the incident plus reflected field, that was given in (17) and (18):

$$\begin{aligned} V_S'(z) &= E_z(z,h) \\ &= E_v \sin\psi \left(e^{jk_0 h \sin\psi} - R_v e^{-jk_0 h \sin\psi} \right) e^{-jk_0 z \cos\psi} \end{aligned} \tag{B4}$$

In addition, the terms V_1 and V_2 in (B3) are the lumped voltage sources at each end due to the y-component of the external field $E_y(y,z)$ (from (20) and (21). Here only V_1, the one in z=0, is considered because the other will be infinitely far away and, hence, not part of the solution, thus

$$V_1 = -\int_0^h E_y(y,0) dy = -E_v \cos\psi h (1+R_v) \tag{B5}$$

where in the evaluation of the integral the same approximation as in (23) was used, (i.e., assuming that h is electrically small). By replacing (B5) in (B3) and then in (B2) it was then shown that V_1 from (B5) is the term that corresponds to the vertical contribution of $V(0)$ in (B2), and that corresponds to V_{oc1} from (23). Finally, by replacing (B4) in (B3) and evaluating the integral analytically for $L \rightarrow \infty$ (with the assumption of $\mathrm{Im}[\gamma]<0$ to assure convergence) as

$$\int_0^\infty e^{j\gamma(L-\zeta)} e^{-j\zeta k_0 \cos\psi} d\zeta = -\frac{je^{jL\gamma}}{\gamma + k_0 \cos\psi}$$

it is found that the term that corresponds to the horizontal contribution of $V(0)$ in (B2) equals V_{oc2}, thus

$$V(0) = V_{oc1} + V_{oc2} \tag{B6}$$

that completes the validation of (26) through the conventional TL theory. It has also been verified that a more general validation holds with finite L, by taking into account the dependence of $E_y(y,z)$ on the vertical coordinate in the calculation of the integral in (B5).

Appendix C

Lossless Line over Perfect Ground

For perfectly conducting earth, $\varepsilon_{r2} \rightarrow 1$, $\sigma_2 \rightarrow \infty$, thus $R_v \rightarrow 1$. Furthermore, for a lossless line $\gamma_{TL} = k_0$ and (26) reduces to

$$V_{oc} = -2E_v h (1+R_v)\cos\psi + \frac{jE_{zv}(0,h)}{(k_0 \cos\psi + \gamma_{TL})} \tag{C1}$$

From (18):

$$\begin{aligned} E_{zv}(x,y) &= E_v \sin\psi \left(e^{jk_0 y \sin\psi} - R_v e^{-jk_0 y \sin\psi} \right) \\ &= 2jE_v \sin\psi \sin(k_0 y \sin\psi) \end{aligned} \tag{C2}$$

A further approximation can be considered for $h << \lambda = 2\pi/k_0$ that leads to

$$E_{zv}(x,y) = 2jE_v k_0 h \sin^2\psi \tag{C3}$$

and replacing (C3) into (C1) it is found:

$$\begin{aligned} V_{oc} &= -2E_v h \cos\psi - \frac{2E_v k_0 h \sin^2\psi}{(k_0 \cos\psi + k_0)} \\ &= -2E_v h \left(\cos\psi - \frac{\sin^2\psi}{(\cos\psi + 1)} \right) = -2E_v h \end{aligned} \tag{C4}$$

An equivalent finding to (C4) is shown in [23], p. 85. This result shows that for a lossless line, and for a distance from the ideal ground plane that is electrically small, the voltage on the line (with zero reference both to ground and infinity) is independent of the frequency and the angle of incidence.